Supplemental Figure

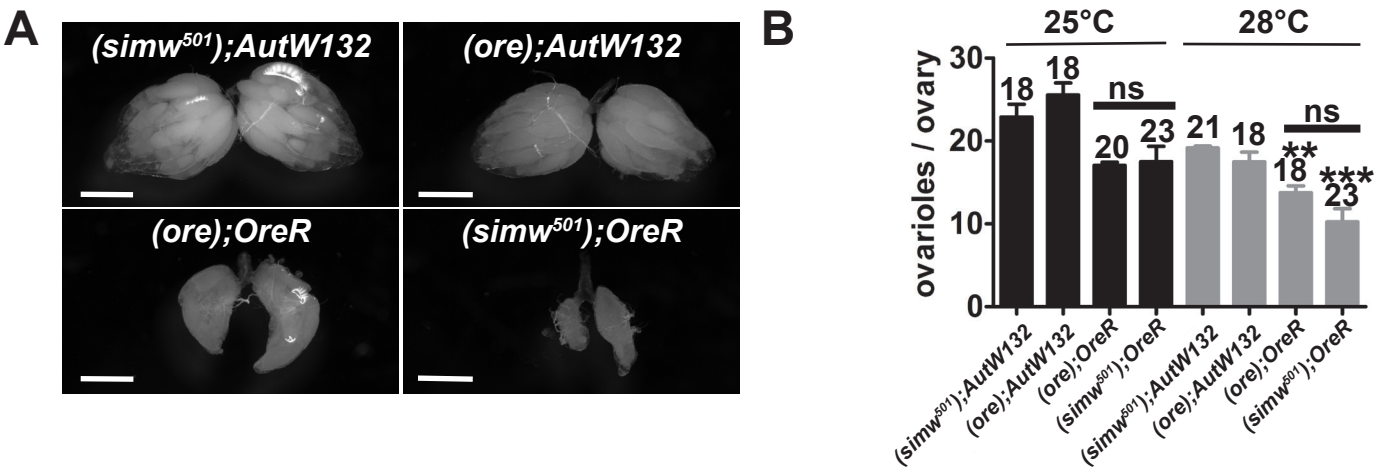

Fig. S1. The *(ore); OreR* and (*simw*^{501}); *OreR* females have smaller ovaries and reduced ovariole numbers at higher temperature. (A) Bright field images of ovaries from the indicated mito-nuclear females that were raised at 28°C. Scale bar: 500µm. (B) Quantification of ovariole numbers from the indicated mito-nuclear females raised at either 25°C (black bars) or 28°C (grey bars). The numbers on the bars represent the total number of ovaries analyzed. Comparing to *(simw*^{501}*); AutW132* at the same temperature, **: $p < 0.01$; *** = $p < 0.001$ by two-way ANOVA. Error bars represent standard error.

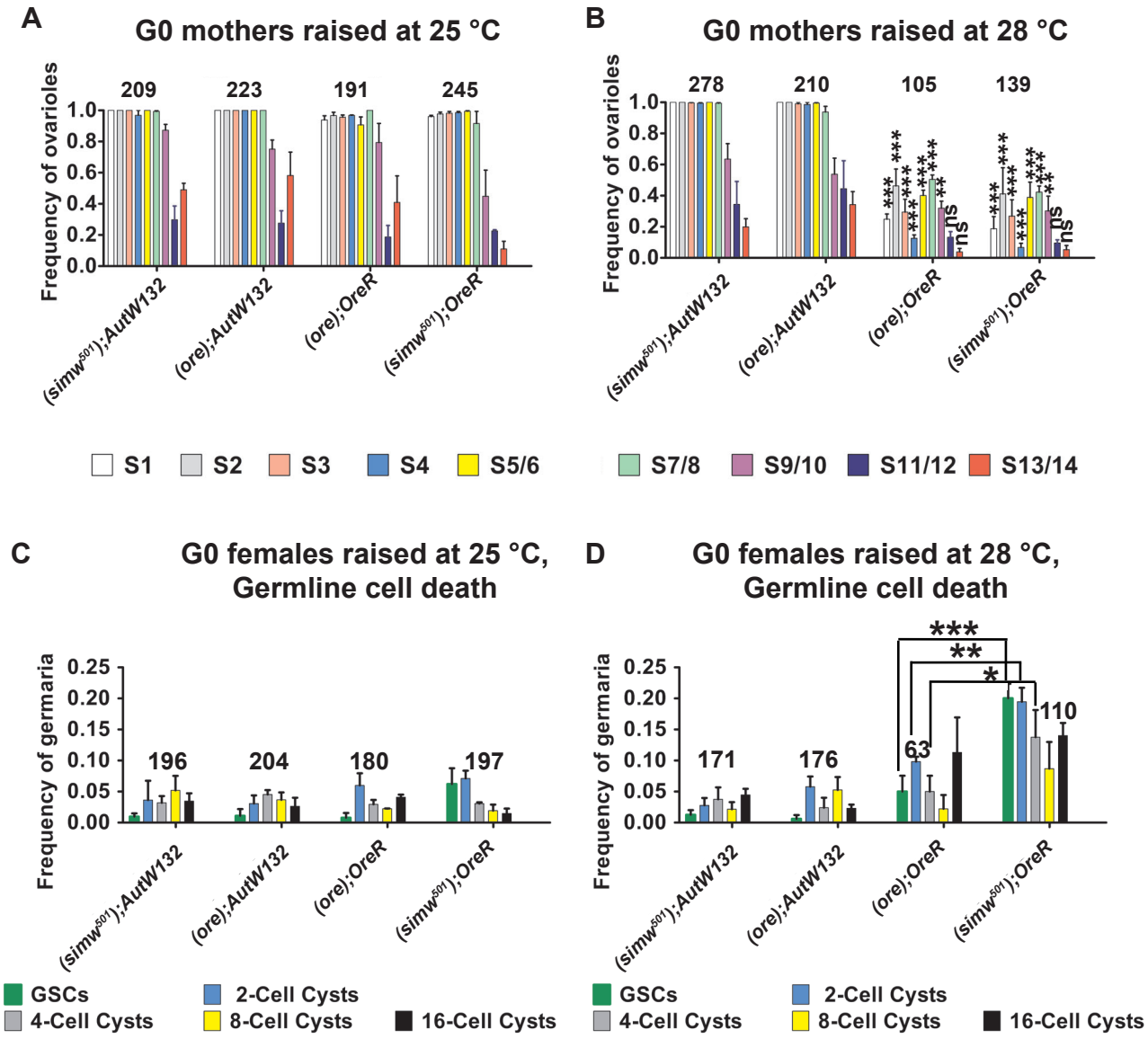

Fig. S2. The *OreR* nuclear genotype contributes to a temperature-sensitive ovarian failure that is enhanced by the incompatible *simw^{501}* mitochondria. (A-B) Quantification of frequency of ovarioles with different stages of egg chambers (earlier to later stages are from left to right) from the indicated mito-nuclear females raised at either 25°C (A) or 28°C (B). The numbers on the bars represent the total number of ovarioles analyzed. Comparing to *(simw^{501}); AutW132* at the same temperature, **: p<0.01; ***: p<0.001. N=3. Error bar represents standard error. (C-D) Quantification of the frequency of germaria with germline cell death from the indicated mito-nuclear females raised at either 25°C (C) or 28°C (D). The y-axis represents the frequency of germaria with germline cell death in cysts comprising the indicated cell numbers (C). The numbers on the bars represent the total number of germaria analyzed. N=3. Error bar represents standard error. Comparison of *(ore); OreR* and *(simw^{501}); OreR* at the same temperature *: p<0.05; **: p<0.01; ***: p<0.001 by two-way ANOVA.

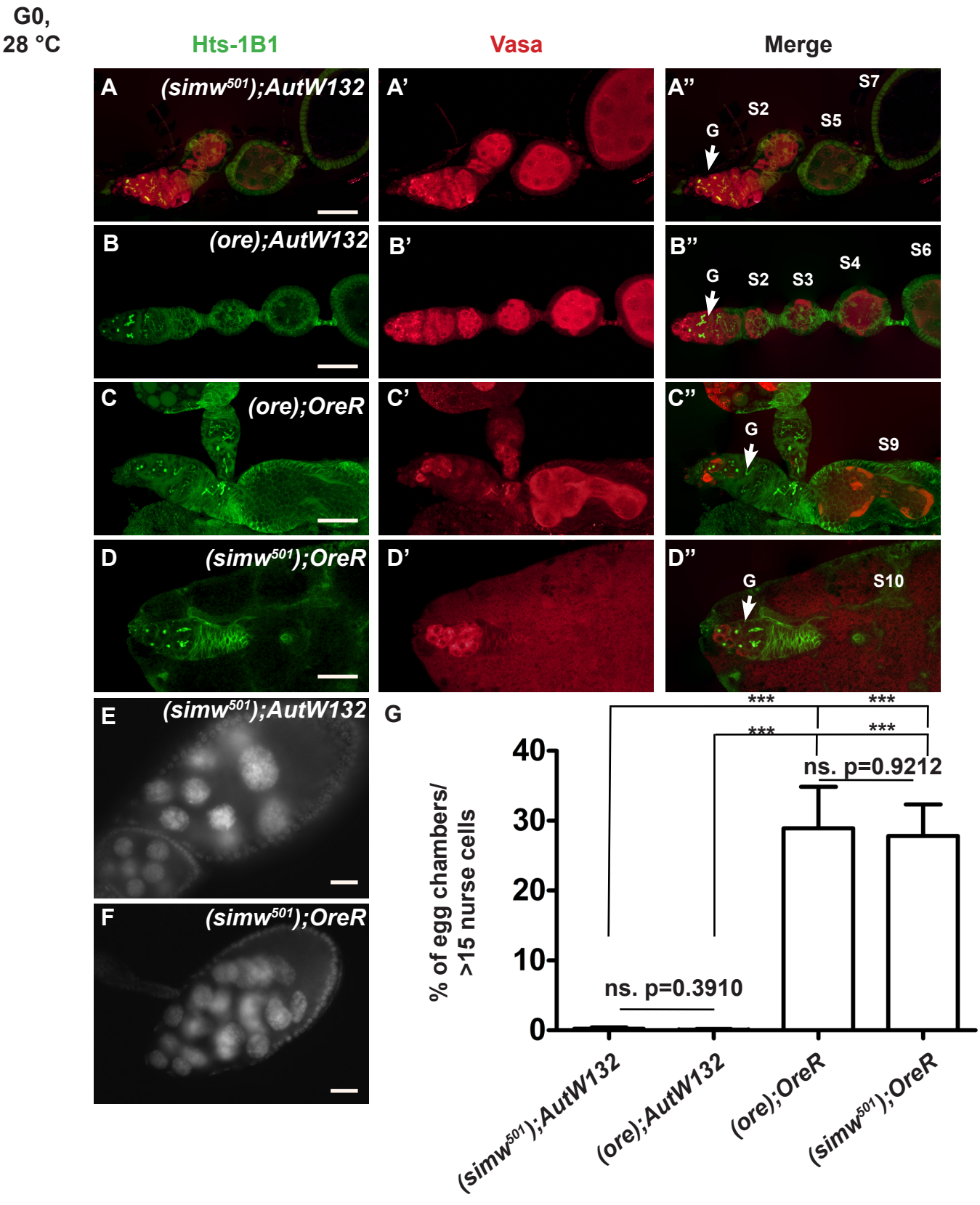

Fig. S3. At 28°C, the *OreR* nuclear genome contributes to the loss-of-germline cells and increased nurse cell number per egg chamber. Confocal images of ovarioles from the indicated mito-nuclear females that were raised at 28°C. The ovarioles were labeled with anti-Hts (A-D, green), anti-Vasa (A'-D', red) and merged (A''-D''). In (D, D', D'') a germarium (G) is directly attached to a stage 10 (S10) egg chamber in a *(simw^{501}); OreR* ovariole. Scale bar: 30µm. (E) A stage 9 egg chamber from *(simw^{501}); AutW132* with 15 nurse cells. (F) A stage 9 egg chamber from *(simw^{501}); OreR* with more than 15 nurse cells. Scale bar: 20µm. (G) Quantification of the percentage of egg chambers with increased number of nurse cells at 28 °C. N=4. Error bar represents standard error. ***: p<0.001.

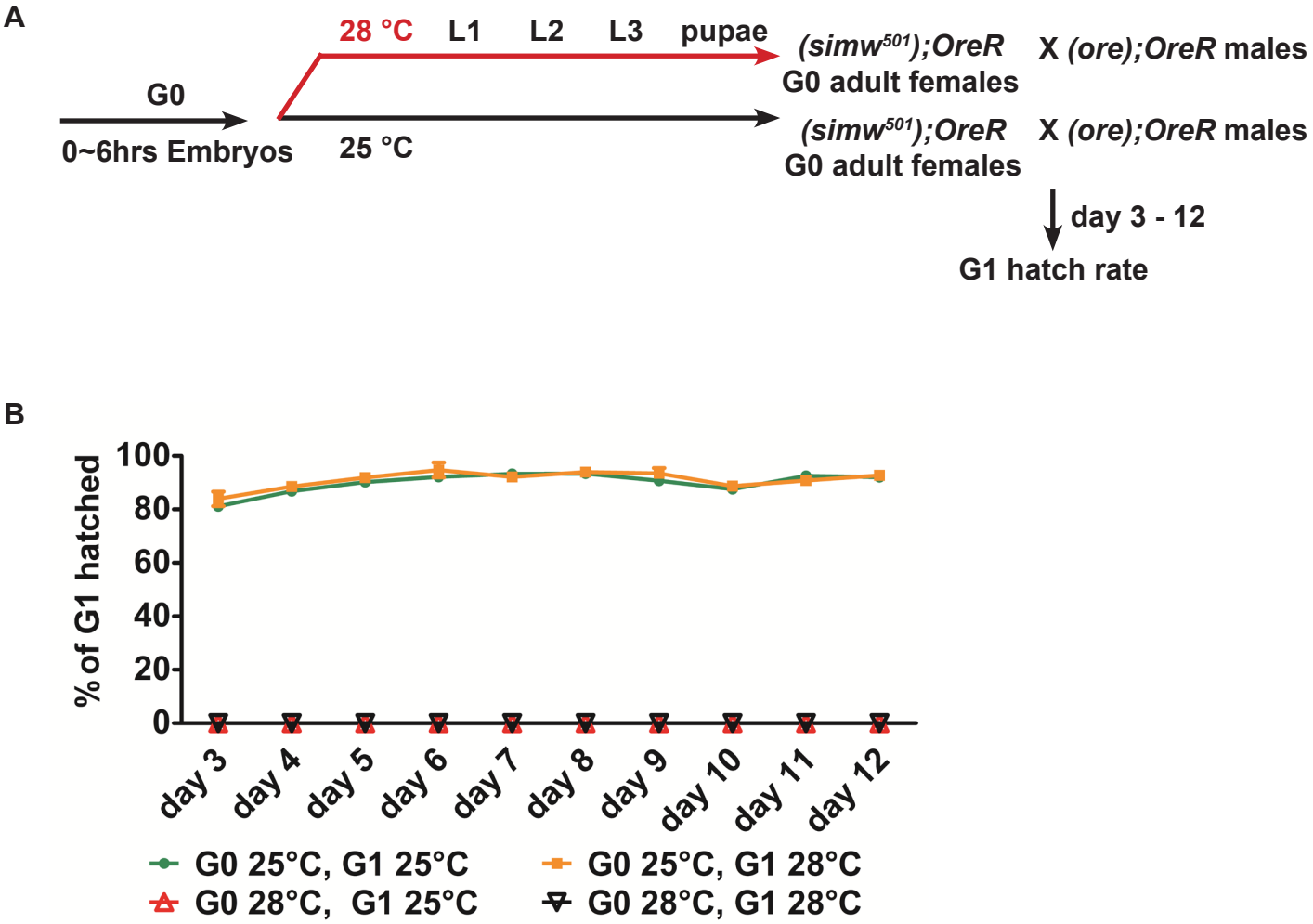

Fig. S4. Homozygous *Aatm*^{275V} G1 embryos from *(simw*^{501}*); OreR* mothers raised at 28°C also have a severely reduced hatch rate. (A) Experimental scheme for temperature shift and female egg lay rate assay. The *(simw*^{501}*); OreR* G0 mothers were raised at 25 °C or 28 °C and then crossed to the fertile *(ore);OreR* males (see Table II for genotypes). Eggs were collected on days 3-12 and allowed to develop at the same temperature, or shifted to the reciprocal temperature, followed by hatch rate counts. (B) G1 embryonic hatch rates. Embryonic hatch rates were measured for mothers of different ages post eclosion (x-axis). Data represents average G1% hatched and standard error for three biological replicates.

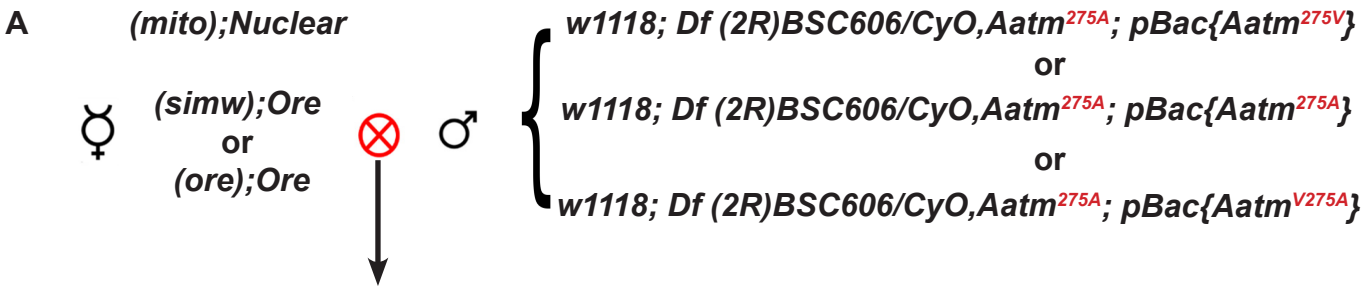

G0 genotypes

		Allele and dosage		
	Mito: (simw) or (ore)	$Aatm^{275V}$	$Aatm^{275A}$	$Aatm^{V275A}$
Nuclear	$Aatm^{275V}/CyO,Aatm^{275A}; phiC31\{Aatm^{275V}\}/+$	2	1	0
	$Aatm^{275V}/Df(2R)BSC606; phiC31\{Aatm^{275V}\}/+$	2	0	0
	$Aatm^{275V}/CyO,Aatm^{275A}; phiC31\{Aatm^{275A}\}/+$	1	2	0
	$Aatm^{275V}/Df(2R)BSC606; phiC31\{Aatm^{275A}\}/+$	1	1	0
	$Aatm^{275V}/CyO,Aatm^{275A}; phiC31\{Aatm^{V275A}\}/+$	1	1	1
	$Aatm^{275V}/Df(2R)BSC606; phiC31\{Aatm^{V275A}\}/+$	1	0	1

Fig. S5. The rescue crosses and genotypes of G0 mothers. *($simw^{501}$); OreR* or *(ore); OreR* virgin females were crossed to males from rescue strains of the indicated genotypes. The red superscript indicates the allele of *Aatm*: $Aatm^{275A}$ (compatible with $simw^{501}$) $Aatm^{275V}$ (incompatible with $simw^{501}$) $Aatm^{V275A}$ (incompatible genomic transgene mutated to compatible allele). The three columns of numbers under each allele on the bottom right indicate the dosage of that allele in the different G0 females. See Fig.3E for the rescue results.

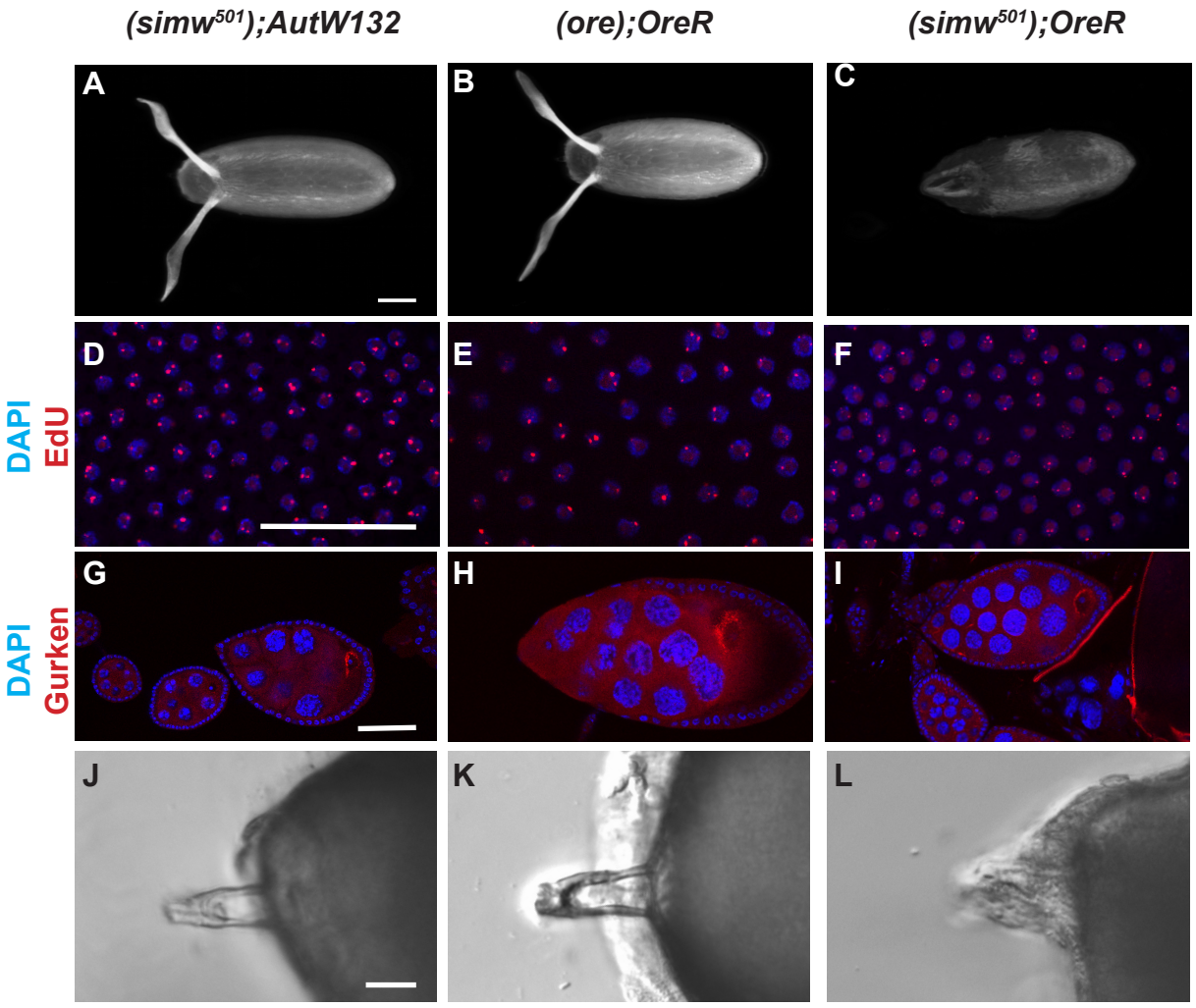

Fig. S6. *(simw^{501}); OreR* mothers raised at 28°C lay eggs with aberrant dorsal appendages and micropyles, but do not have altered Gurken protein localization or developmental gene amplification. Eggs and ovaries were analyzed from females raised at 28 C and of the genotype indicated at the top of each column: *(simw^{501}); AutW132* (A, D, G, J), *(ore); OreR,* (B, E, H, K), *(simw^{501}); OreR* (C, F, I, L). (A-C) Bright field images of laid eggs viewed from a dorsal aspect. Eggs from *(simw^{501}); OreR* females are shorter, with unusual dorsal appendage morphology. Scale bar:100µm**.** (D-F) Confocal images of EdU-labeled amplicon foci in stage10B follicle cells. Scale bar: 50µm. (G-I) Confocal images of anti-Gurken labeled egg chambers. Scale bar;50µm. (J-L): Differential Interference Contrast (DIC) images of micropyles at the anterior of laid eggs. Chorion obscures the micropyle on the egg from the *(simw^{501}); OreR* female (L). Scale bar:15µm.

Table S1. Strains used in this study

(simw^{501});AutW132
(ore);AutW132
(ore);OreR
(simw^{501});OreR
w^{1118}; Df(2R)BSC606 / CyO,Aatm^{275A}; PBac{Aatm^{275V}}
w^{1118}; Df(2R)BSC606 / CyO,Aatm^{275A}; PBac{Aatm^{275A}}
w^{1118}; Df(2R)BSC606/ CyO,Aatm^{275A}; PBac{Aatm^{V275A}}
y w^{67c23} (Bloomington stock #6599)

Strains were previously described by Meiklejohn et al. 2013 and are available upon request.